# Polymer Chemistry

Accepted Manuscript






ROYAL SOCIETY OF CHEMISTRY

www.rsc.org/polymers

# Effects of Rigid Core and Flexible Tails on the Phase Behaviors of Polynorbornene-Based Mesogen-Jacketed Liquid Crystalline Polymers

Zhen-Yu Zhang, Qian Wang, Ping-Ping Hou, Zhihao Shen,* and Xing-He Fan*

Beijing National Laboratory for Molecular Sciences, Key Laboratory of Polymer Chemistry and Physics of Ministry of Education, Center for Soft Matter Science and Engineering, College of Chemistry and Molecular Engineering, Peking University, Beijing, 100871, China

* To whom the correspondence should be addressed. E-mail: fanxh@pku.edu.cn (X.-H.F.); zshen@pku.edu.cn (Z.S.).

**Abstract:** A new series of mesogen-jacketed liquid crystalline polymers (MJLCPs) with a polynorbornene main chain and different side groups were prepared by ring-opening metathesis polymerization. The liquid crystalline (LC) phase behaviors of these polymers were investigated by differential scanning calorimetry, polarized light microscopy, and wide-angle X-ray diffraction. Depending on the rigid side-chain core and peripheral alkyl chains, these polymers show different LC structures. The polymer with the terphenyl rigid side-chain core and relatively short alkyl tails is amorphous in the whole temperature range, while those with the same rigid side-chain core but longer alkyl tails exhibit columnar nematic ($Col_n$) phases. Polymers with a longer rigid side-chain core and relatively long alkyl tails develop into smectic A (SmA) phases.

In addition, the LC polymers obtained in this study display LC phases in wide temperature ranges.

## Introduction

Liquid crystalline polymers (LCPs) are important functional polymers with ordered structures,[1-5] and they are useful in information technology,[6,7] medical applications,[8] and materials science.[9-11] Their properties are not only strongly influenced by the chemical structures of the polymers themselves, but also deeply dependent on the self-assembled physical structures of the polymer chains.[12-16]

In the development of side-chain LCPs (SCLCPs), the decoupling concept proposed by Finkelmann *et al*. in 1978 is extremely important.[17,18] The flexible spacers between the side-chain mesogen and the backbone decouple the motions of mesogens and main chains, facilitating the formation of liquid crystalline (LC) phases. On the other hand, Zhou *et al*. developed a new type of LCPs, namely mesogen-jacketed LCPs (MJLCPs), in the late 1980s.[19,20] In these polymers, bulky side groups are laterally attached to the main chain through a single C-C bond or a short spacer.[3,21] The "jacketing" effect owing to steric reasons forces the main chain to take an extended-chain conformation, and thus MJLCPs have physical properties similar to main-chain LCPs, although chemically they are side-chain type polymers.[3] For MJLCPs, the polymer chains serve as supramolecular mesogens to construct ordered LC structures. Many MJLCPs have been reported, with monomers derived from 2-vinylhydroquinone,[19,20,22,23] 2-vinylterephthalic acid (VTA),[24-26] vinylbiphenyl,[27-29] vinylterphenyl,[30,31] and so on. Many LC

phases have been observed, including hexagonal columnar ($Col_h$),[26,29] columnar nematic ($Col_n$),[30,32] hexatic columnar nematic ($Col_{hn}$),[32,33] smectic A (SmA),[27,34] smectic C,[28,35] and so forth.

Most MJLCPs have been synthesized by free radical polymerization. However, due to the steric effect of huge pendant groups, MJLCPs with high molecular weights (MWs) are difficult to obtain by using this approach. In addition, some monomers, such as those with fullerene (C60), cannot be polymerized by free radical polymerization.[36] Recently a new type of living polymerization method, ring-opening metathesis polymerization (ROMP), has been developed.[37-44] Norbornene monomers can be easily synthesized, and the corresponding polymers with high MWs and relatively narrow MW distributions can be obtained through ROMP. Recently Yang *et al*. reported a series of polynorbornene-based MJLCPs that formed smectic phases only when the number of carbon atoms in the alkoxyl terminal chains was more than nine.[40] Zhu *et al*. synthesized a new series of MJLCPs with polynorbornene as the main chain, PNb*n*PT (*n* is the number of carbons in the side-chain alkyl tails, and *n* = 8, 10, 12, 14, 16, 18).[45] When *n* is large enough, the polymer develops into the SmA phase. This kind of polymer is expected to have great tolerance of functional groups like C60.

In this work, in order to understand the influences of the lengths of the rigid core and the peripheral alkyl chain on the LC phase behavior, we designed a series of polynorbornene-based mesogen-jacketed polymers with different rigid side-chain cores and different peripheral alkyl chains. The polymers were prepared by ROMP. Then we investigated the relationship between the LC phase behaviors and the chemical structures of these polymers.

## Experimental

**Materials and characterization methods.** Dichloromethane ($CH_2Cl_2$) was pretreated by the Braun solvent purification system. *cis*-5-Norbornene-*exo*-2,3-dicarboxylic anhydride (96%) and *N*,*N*-dimethylformamide (DMF, HPLC) were purchased from J&K Chemical. Grubbs' catalyst (third generation) was purchased from Sigma-Aldrich. All other reagents were obtained from commercial sources and used as received unless otherwise noted. $^1$H NMR (400 MHz), high-resolution mass spectrometry (MS), elemental analysis (EA), gel permeation chromatographic (GPC) measurements, thermogravimetric analysis (TGA), differential scanning calorimetry (DSC), polarized light microscopy (PLM), and one-dimensional (1D) wide-angle X-ray diffraction (WAXD) experiments were performed according to the procedures described previously.[46,47] In the DSC experiments, all samples were first heated to 300 $^o$C to eliminate thermal history. For PLM examination, all samples were prepared from powders. For 1D WAXD experiments, about 35 mg of the powder sample was dissolved in tetrahydrofuran (THF, ~1 mL) and cast into a film on a copper substrate. Solvent was then allowed to evaporate at ambient temperature for hours, and the sample was dried at 35 $^o$C in vacuum overnight before characterization. To avoid thermal degradation, the sample chamber was charged with nitrogen during measurements. Two-dimensional (2D) WAXD experiments were performed using a Bruker D8Discover diffractometer with VANTEC 500 as a 2D detector.

**Synthetic procedures.** The chemical structure and synthetic procedure of the monomer

precursor *N*-(4′,4″-bis(*p*-carboxylphenyl)-terphenyl)-2′-*cis*-5-norbornene-*exo*-2,3-dicarboximide (NbTpA) are illustrated in Scheme 1, and the experimental details are described in the Electronic Supplementary Information (ESI).

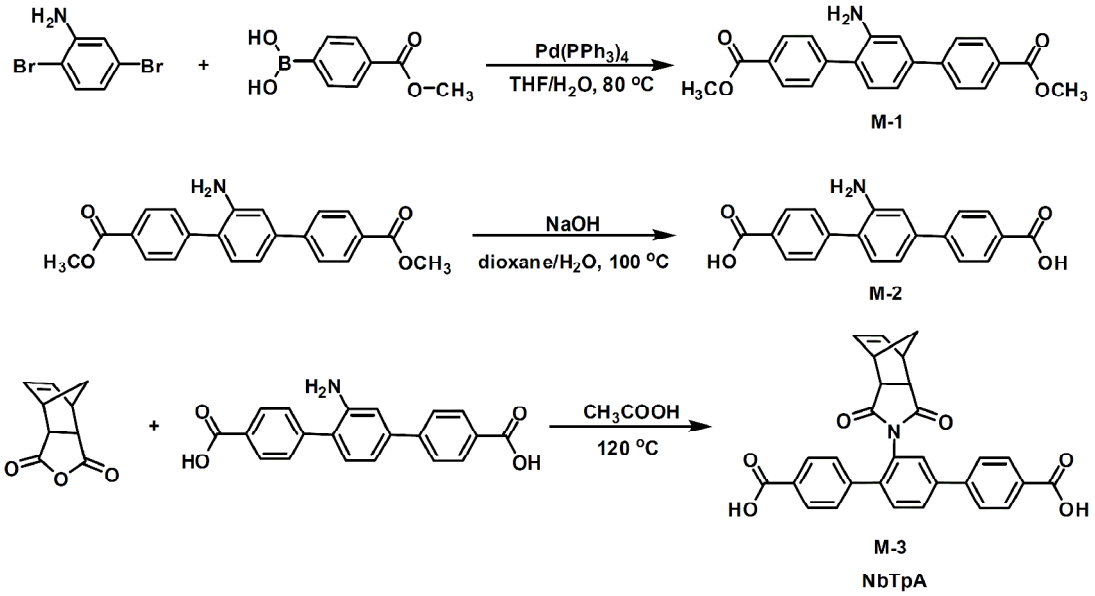


Scheme 1 Synthetic pathway of the precursor NbTpA.

*Synthesis of NbTpCn monomers.* The NbTpC*n* monomers with terphenyl as the rigid core of the mesogenic unit were synthesized as in the example of NbTpC16 as described in the ESI. The preparation methods of the other two monomers (NbTpC8 and NbTpC12) are similar. Scheme 2 shows the chemical structures and synthetic procedures of the monomers.

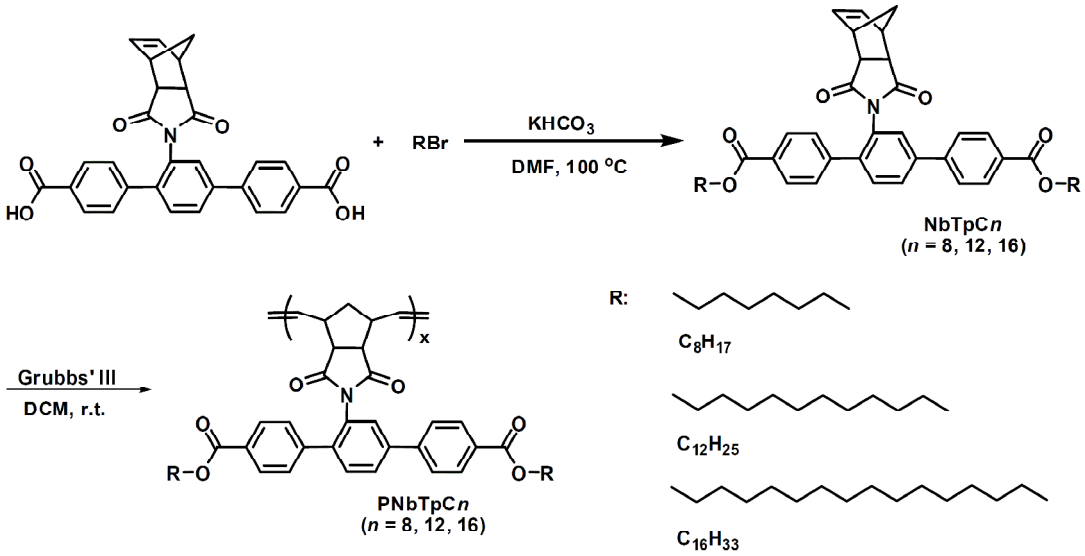


Scheme 2 Synthetic pathway of the NbTpC*n* monomers and the corresponding PNbTpC*n* polymers.

*Synthesis of NbFpCn monomers.* The NbFpC*n* monomers with five benzene rings as the rigid core of the mesogenic unit were synthesized as in the example of NbFpC16 as described in the ESI, with the *p*-(*n*-alkoxyl) phenols prepared according to the method described previously.[48] The preparation method of the monomer NbFpC10,6 is similar. Scheme 3 shows the chemical structures and synthetic procedures of the monomers.

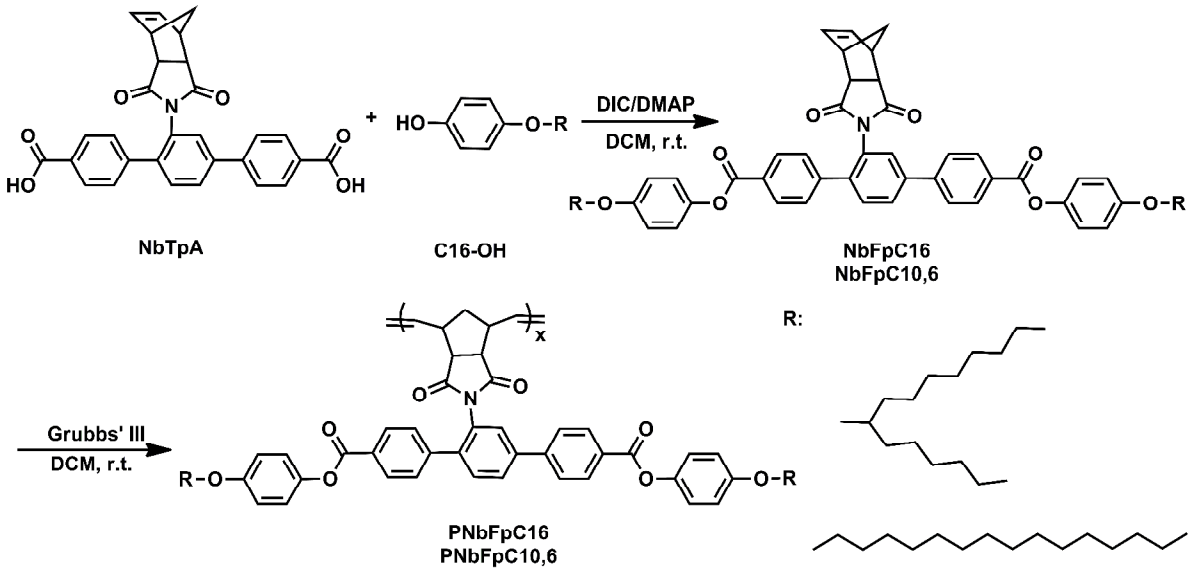


Scheme 3 Synthetic pathway of the NbFpC16 and NbFpC10,6 monomers and the corresponding PNbFpC16 and PNbFpC10,6 polymers.

*Synthesis of polymers.* The synthetic procedures for the polymers with different rigid cores or alkyl peripheral chains are similar. All the polymers were obtained by ROMP using the third-generation Grubbs' catalyst, as shown in Schemes 2 and 3 which also illustrate the chemical structures of the polymers. The details are described below with PNbTpC16 as an example. Starting from their corresponding monomers, PNbTpC8, PNbTpC12, PNbFpC16, and PNbFpC10,6 were similarly prepared as white solids with yields of 95, 90, 95, and 90%, respectively.

NbTpC16 (200 mg) and Grubbs' third-generation catalyst (1.59 mg) were added in a dry Schlenk tube. After three pump-purge cycles with high-purity nitrogen, $CH_2Cl_2$ (~2 mL) was injected into the mixture by using a syringe, and polymerization reaction was initiated. After the reaction mixture was stirred at ambient temperature for 3 h, a few drops of vinyl ethyl ether were

added into the reaction mixture. Then polymerization was stopped in an hour. The mixture was diluted with 5 mL of $CH_2Cl_2$, and then the polymer was precipitated out in 100 mL of methanol. By filtration and drying in vacuum at 35 $^oC$ for 24 h, the target polymer PNbTpC16 was obtained as a white solid. Yield: 95%.

## Results and discussion

**Synthesis of monomers and polymers.** As shown in Schemes 1, 2, and 3, monomers were obtained through multiple steps. In order to investigate the influence of the size of the rigid core and the structure of the peripheral alkyl chain on the LC behavior of the polymer, we designed and synthesized a series of monomers with two rigid cores of different sizes and various peripheral alkyl chains. The key precursor for the two kinds of MJLCPs is NbTpA. In order to obtain NbTpA with a high purity, we chose the synthetic route shown in Scheme 1, although the efficiency of this Suzuki reaction was not high. The reaction of *cis*-5-norbornene-*exo*-2,3-dicarboxylic anhydride and 2′-amino-(4′,4″-bis(*p*-dicarboxylic acid)-terphenyl) readily occurred with a yield of 80%.

The polymers were prepared by ROMP using a third-generation Grubbs' catalyst, with high MWs and relatively narrow MW distributions. The characteristics of these polymers are summarized in Table 1. The number-averaged molecular weight ($M_n$) values of the polymers can be controlled by varying the feeding ratios. Polydispersity indexes (PDIs) of the polymers are in the range of 1.08–1.17, which indicates good control of the polymerization. Figure 1 shows the $^1H$ NMR spectra of NbFpC16 and PNbFpC16 in $CDCl_3$. The characteristic resonances of vinyl H

appearing at $\delta$ = 6.20–6.30 ppm disappear after polymerization, and the resonance peaks of PNbFpC16 at $\delta$ = 5.20–5.75 ppm are rather broad and consistent with the expected polymer structure, indicating the successful polymerization. Figure 2 gives the GPC curves of all the polymers.

Table 1 Molecular characteristics and thermal properties of the polymers

| Polymer | [Monomer]:[Catalyst] | $M_n$ ($\times 10^4$ Da) [a] | PDI [a] | $T_d$ ($^oC$) [b] | $T_g$ ($^oC$) [c] | $T_{transition}$ ($^oC$) [c] |
|---|---|---|---|---|---|---|
| PNbTpC8 | 100:1 | 5.38 | 1.17 | 375 | 122 | – |
| PNbTpC12 | 100:1 | 5.22 | 1.11 | 370 | 113 | – |
| PNbTpC16 | 100:1 | 6.64 | 1.08 | 372 | 111 | – |
| PNbFpC16 | 100:1 | 7.93 | 1.11 | 410 | – | 283 |
| PNbFpC10,6 | 100:1 | 7.66 | 1.14 | 415 | 123 | 238 |

[a] Determined by GPC in THF using polystyrene standards.

[b] 5% weight loss temperature evaluated by TGA under a nitrogen atmosphere at a heating rate of 10 $^o$C/min.

[c] Evaluated by DSC during the second heating cycle at a rate of 20 $^o$C/min.

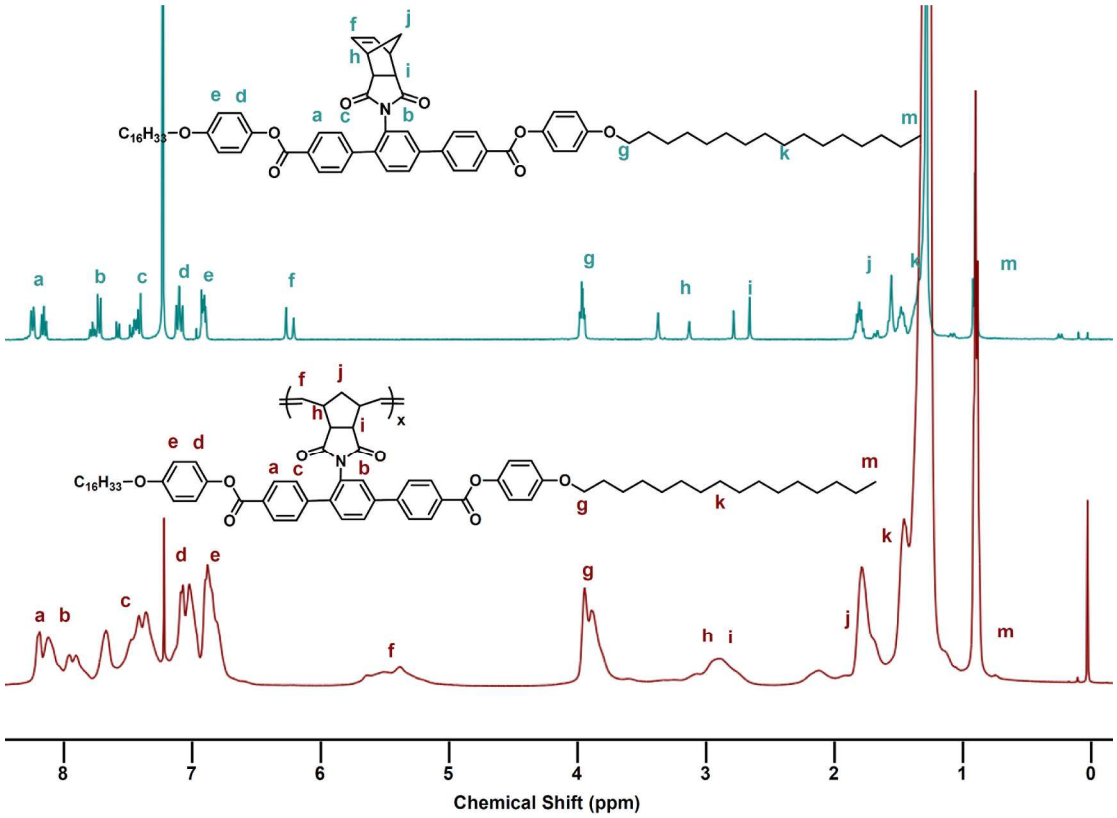


Fig. 1 $^{1}$H NMR spectra of NbFpC16 (top) and PNbFpC16 (bottom) in $CDCl_3$.

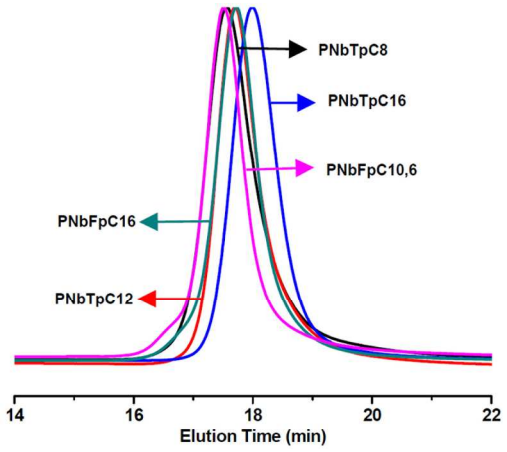


Fig. 2 GPC curves of all the polymers.

**Thermal properties of polymers.** TGA results indicate that all the polymers exhibit excellent thermal stabilities. The 5% weight loss temperatures are all above 370 $^{o}$C in a nitrogen

atmosphere, as shown in Table 1 and Fig. S8 (ESI).

Figure 3 shows the DSC traces of the polymers during the first cooling processes at a rate of 3 $^{o}$C/min and the second heating processes at a rate of 20 $^{o}$C/min under a nitrogen atmosphere. Glass transition temperature ($T_g$) of PNbTpC12 is 113 $^{o}$C. The glass transition of PNbFpC16 with a longer rigid core can not be detected in the DSC experiment, possibly because of the increased rigidity of the mesogenic unit which leads to a quite slow glass-transition kinetics of the polymer. The $T_g$ value of PNbFpC10,6 with branched peripheral alkyl chains is 123 $^{o}$C, as shown in Fig. 3c. The DSC traces of PNbTpC8 and PNbTpC16 are similar to those of PNbTpC12, and the $T_g$ values are 122 $^{o}$C and 111 $^{o}$C, respectively, as shown in Table 1 and Fig. S9 (ESI).

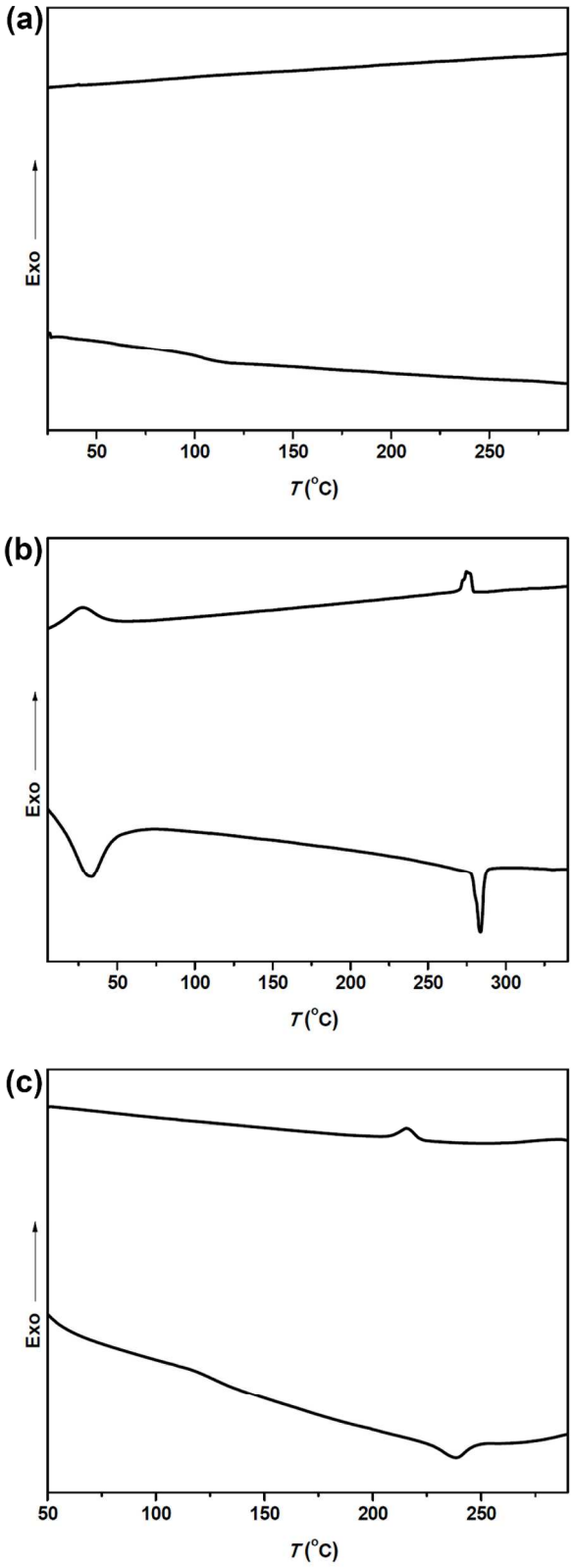


Fig. 3 DSC traces of PNbTpC12 (a), PNbFpC16 (b), and PNbFpC10,6 (c) during the first

cooling processes at a rate of 3 $^{o}$C/min and the second heating processes at a rate of 20 $^{o}$C/min under a nitrogen atmosphere.

No transition peaks can be observed in the DSC thermograms of PNbTpC12. During heating, one endothermic peak emerges at 238 $^{o}$C and 283 $^{o}$C for PNbFpC10,6 and PNbFpC16, respectively. And the enthalpic changes of these transitions are relatively small. Such a transition may be related to the isotropization of the polymer from an LC phase. For PNbFpC16, the transitions below 50 $^{o}$C can be attributed to the melting and crystallization of the alkyl tails in the side chain.

**Phase structures of polymers.** The mesomorphic behaviors of these polymers were then examined by PLM and 1D/2D WAXD techniques. The PLM results are consistent with DSC results. For PNbTpC12 and PNbTpC16, no birefringence was observed in the whole temperature range during the experiments (Fig. S10 in ESI). Figure 4 illustrates the textures of PNbFpC16 and PNbFpC10,6 at 150 $^{o}$C. For PNbFpC16, strong birefringence was observed at ambient temperature, and the birefringence disappeared at 300 $^{o}$C during the heating process. During the cooling process, birefringence reappeared at 285 $^{o}$C. For PNbFpC10,6, the phenomenon is similar to that of PNbFpC16, and its clearing temperature is about 250 $^{o}$C.

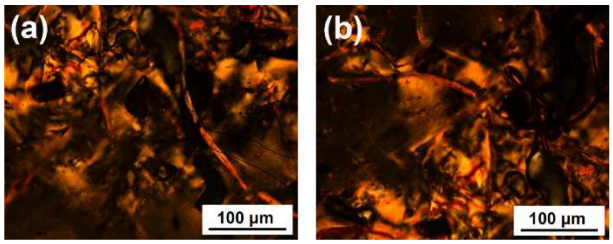


Fig. 4 PLM micrographs of PNbFpC16 (a) and PNbFpC10,6 (b) at 150 $^{o}$C

Because the information from DSC and PLM experiments was not sufficient to determine the phase structures of the polymers, variable-temperature 1D WAXD experiments during the first heating and cooling on solution-cast samples were performed. These polymers show three types of behaviors in 1D WAXD experiments. For PNbTpC8 (Fig. 5), only two broad halos in the low- and high-angle regions can be observed at all temperatures during the heating and cooling processes. These results indicate the amorphous nature of PNbTpC8.

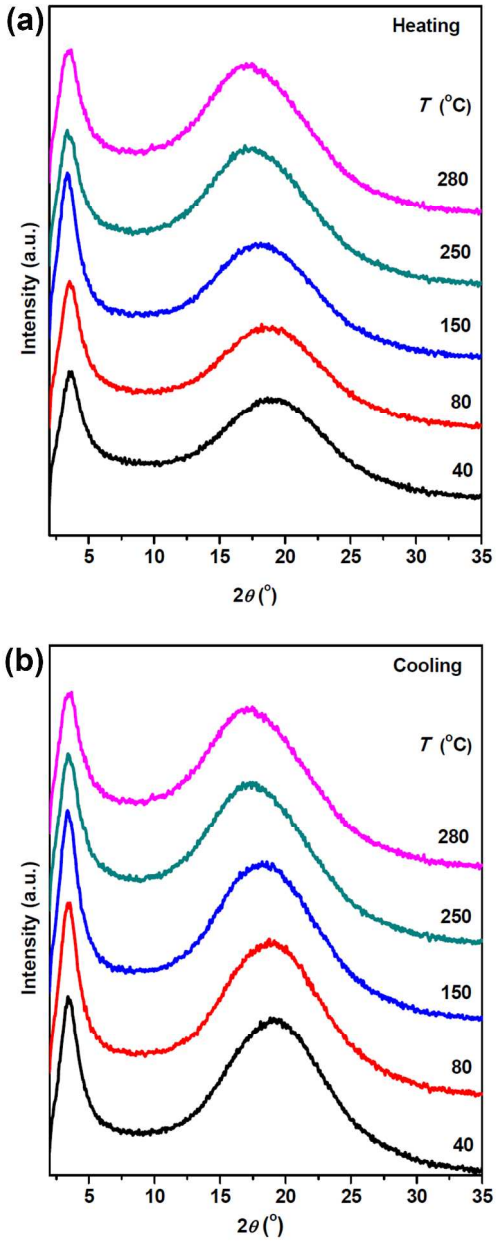


Fig. 5 1D WAXD profiles of PNbFpC8 during the first heating (a) and the subsequent cooling (b) processes.

For PNbTpC12 (Fig. S11 in the ESI) and PNbTpC16 (Fig. 6), a diffraction peak in the low-angle region and a broad halo in the high-angle region can be observed at ambient temperature. The intensity of the diffraction peak becomes lower during the first heating process

and becomes higher again during the subsequent cooling process. This diffraction peak indicates a possible $Col_n$ phase in the whole temperature range, although in the PLM experiments, these two polymers did not show birefringence. The broad halo in the high-angle region is the typical amorphous halo attributed to the amorphous packing of the alkyl side-chain tails and the average lateral distance between the side-chain mesogens. The *d*-spacing values of PNbTpC12 and PNbTpC16 are 3.00 nm and 3.45 nm, respectively. The side-chain lengths of these two polymers can be estimated as 4.35 nm and 5.37 nm, respectively, with the assumption of an all-*trans* conformation of the alkyl chains. The significant differences between the *d*-spacing values and the estimated side-chain lengths are attributed to the deviation from the all-*trans* conformation, tilting of the side chains with respect to the backbone, and partial interdigitation of the peripheral alkyl chains.

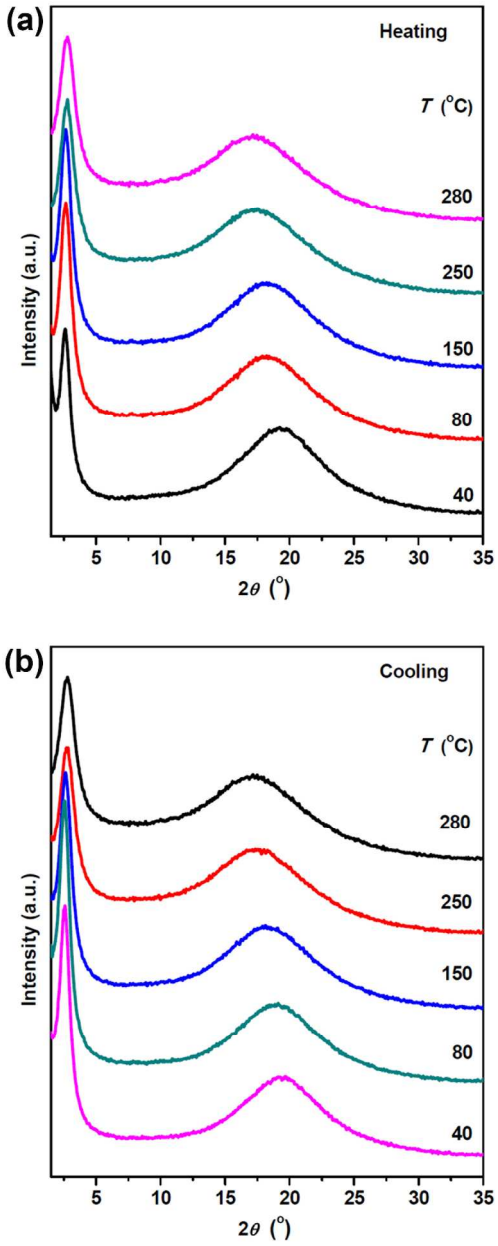


Fig. 6 1D WAXD profiles of PNbTpC16 during the first heating (a) and the subsequent cooling (b) processes.

For PNbFpC16 (Fig. 7), a diffraction peak in the low-angle region and a broad halo in the high-angle region can be observed at ambient temperature. The diffraction peak becomes much stronger in intensity and much sharper during the first heating process. This sharp diffraction

peak indicates a smectic phase that retains during the subsequent cooling process.[40] The *d*-spacing value of PNbFpC16 is 4.77 nm, which is also significantly lower than the estimated side-chain length of 6.40 nm (assuming an all-*trans* conformation). Again, the possible reason for the difference is similar to that of PNbTpC12. To aviod sample degradation, we did not test at temperatures higher than 250 $^{o}$C. However, the transition at 283 $^{o}$C during heating in the DSC thermogram of PNbFpC16 (Fig. 3b) may be related to the isotropization of the smectic phase, which can be deduced from the phase behavior of PNbFpC10,6.

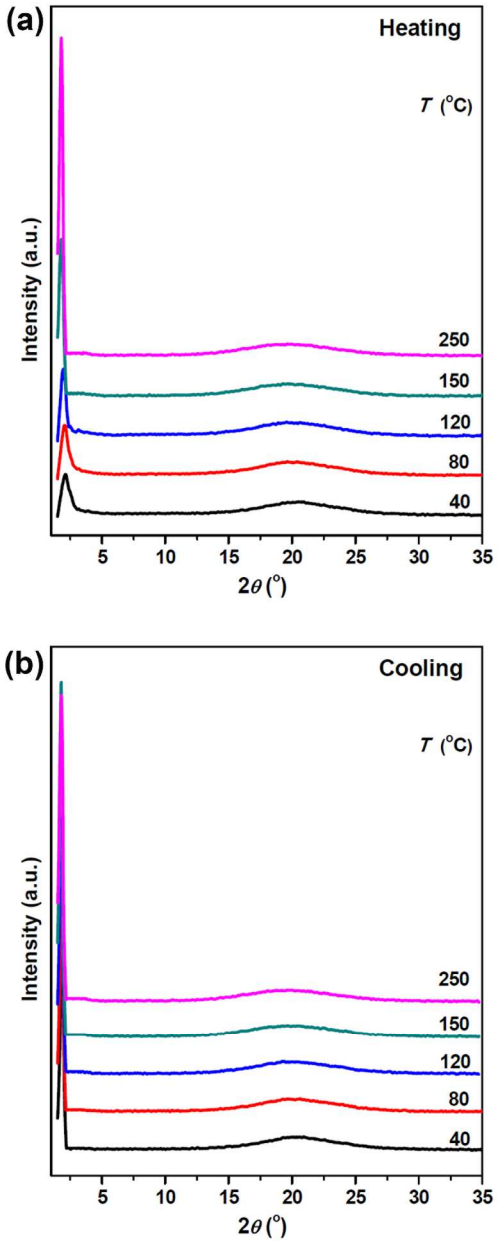


Fig. 7 1D WAXD profiles of PNbFpC16 during the first heating (a) and the subsequent cooling (b) processes.

For PNbFpC10,6 (Fig. 8), the 1D WAXD results are similar to those of PNbFpC16. The sharp diffraction peak in the low-angle region indicates a smectic phase. However, the diffraction peak disappears at a high temperature of 280 °C during the heating process, indicating the

isotropization of the LC phase. Upon cooling, the sharp diffraction peak appears again at about 240 $^{o}$C. These results are consistent with the DSC data. The *d*-spacing values of PNbFpC10,6 is 4.24 nm, smaller than the estimated side-chain length of 4.92 nm (assuming an all-*trans* conformation). The difference between the *d*-spacing value and the estimated side-chain length is also owing to the deviation from the ideal conformation, tilting of the side chain, and partial interdigitation.

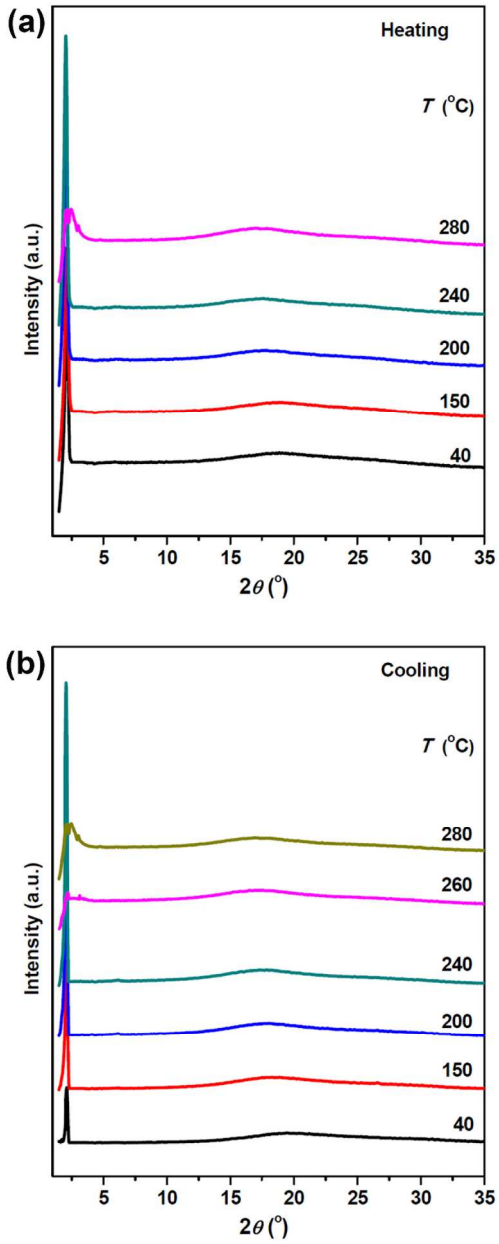


Fig. 8 1D WAXD profiles of PNbFpC10,6 during the first heating (a) and the subsequent cooling (b) processes.

In order to confirm or determine the LC phase structures, 2D WAXD experiments were performed at ambient temperature. Parts a and b of Fig. 9 show the 2D WAXD patterns of PNbTpC16. When the X-ray incident beam is perpendicular to the shear direction (meridian

direction), a pair of sharp diffraction arcs at $2\theta$ = 2.56° (*d*-spacing of 3.45 nm) appear on the equator, and the high-angle amorphous halo centers along the meridian, as shown in Fig. 9a. Figure 9b gives the 2D WAXD pattern with the X-ray incident beam parallel to the shear direction. A ring pattern at $2\theta$ = 2.56° (*d*-spacing of 3.45 nm) can be observed. These two patterns indicate that the LC phase of PNbTpC16 can be identified as $Col_n$.[30] The LC phase of PNbTpC12 is also $Col_n$, as shown in Fig. S12 (ESI).

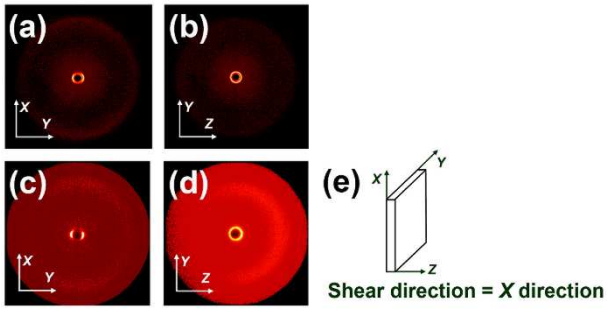


Fig. 9 2D WAXD patterns of PNbTpC16 with the X-ray beam perpendicular (a) and parallel (b) to the shear direction, those of PNbFpC16 with the X-ray beam perpendicular (c) and parallel to the shear direction (d), and the shear geometry (e).

Parts c and d of Fig. 9 are the 2D WAXD patterns of PNbFpC16 with the X-ray incident beam perpendicular and parallel to the shear direction, respectively. A pair of diffraction arcs with a *d*-spacing value of 4.77 nm appear on the equator in Fig. 9c, while the high-angle amorphous halos are centered on the median. This pattern along with the 1D WAXD results demonstrates that PNbFpC16 exhibits a SmA phase, which eliminates the possibility of the tilting of the side chain among the reasons for the large difference in the *d*-spacing value (4.77 nm) and the estimated side-chain length (6.40 nm). Therefore, the alkyl chain ends in the side

groups are packed in a significantly interdigitated manner. Thus, the SmA phase is actually a partial double layer SmA ($SmA_d$) phase. Figure 9d shows a low-angle diffraction ring, and the amorphous halo also appears as a diffuse ring, confirming the SmA phase of PNbFpC16. The LC phase of PNbFpC10,6 is similar to that of PNbFpC16, which is also an SmA phase, as shown in Fig. S12 of the ESI.

As shown in Fig. 10, the phase behaviors of the polymers are different. Compared with the polymer PNb16PT in our previous work,[45] the subtle difference in the rigid side-chain cores of PNb16PT and PNbTpC16 leads to remarkably different phase structures. PNbTpC16 containing a terphenyl core shows a $Col_n$ phase, while PNb16PT with a longer rigid side-chain core also containing three benzene rings but connected by two ester linkages exhibits a SmA phase. Such a trend for the formation of SmA phases with increasing rigidity or length of the side chain has been observed in many MJLCP systems,[3] although the increase in the *d*-spacing value from PNbTpC16 (3.45 nm) to PNb16PT (3.60 nm) is only about 0.15 nm. For PNbFpC16 with an even longer rigid side-chain core, it also displays a SmA phase, as expected. In addition, the change of the architecture of the peripheral alkyl chain from a linear one to a branched one decreases the $T_g$ and the clearing temperature of the polymer containing five benzene rings in the side chain and long enough alkyl tails, while the LC structure remains the same. Similar to MJLCP systems we have studied previously, the following chemical aspects should be pointed out for the formation of LC phases in these polymers. First, in order to have a balance of rigid and flexible components, relatively long peripheral alkyl chains are needed in these polymers.[45] In addition, because of the larger distance between neighboring mesogenic units along the

backbone in these polynorbornene-based MJLCPs compared with that in traditional MJLCPs with a polystyrene main chain, rigid cores with relatively larger sizes are needed in the side chains.[45] Finally, with a further increase in the size of the rigid core for PNbFpC16 and PNbFpC10,6, the polymers become ribbon-like in shape and form SmA phases owing to the parallel packing of the mesogenic groups.[27,34]

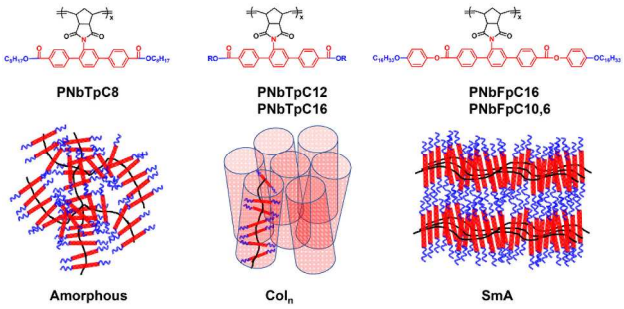


Fig. 10 Schematic drawing of the phase structures of the polymers.

## Conclusions

We synthesized a new series of MJLCPs with polynorbornene as the main chain and terphenyl as the central core in the side-chain mesogenic unit. The lengths of the rigid core and the alkyl tails in the side chain strongly affect the LC properties of the resulting polymers. With long enough peripheral alkyl chains, the polymer exhibits a $Col_n$ phase. Increasing the size of the rigid side-chain core renders polymers that form SmA phases. The temperature ranges of the LC phases of all these new MJLCPs are wide (30–300 $^oC$). In addition, varying the architecture of the peripheral alkyl chain with a sufficient length from linear to branched lowers the $T_g$ and isotropization temperature of the polymer containing the longer rigid side-chain core, without changing the phase structure. Because of the good control in MWs and MW distributions offered

by ROMP, these polynorbornene-based MJLCPs displaying various stable LC phases have potential applications as building blocks in block copolymers or as functional materials.

**Electronic supplementary information (ESI) available:** Synthesis of monomers and their precursors; $^{1}$H NMR spectra of monomers and polymers; TGA curves of all polymers; PLM micrographs and DSC curves of PNbTpC12 and PNbTpC16; 1D WAXD profiles of PNbTpC16.

**Acknowledgments**

The anthors acknowledge the support from the National Natural Science Foundation of China (Grants 21574001, 21134001 and 21374002). The authors also thank the Shanghai Synchrotron Radiation Facility for the assistance with the WAXD experiments.

**Notes and references**

1 P. Davidson, *Prog. Polym. Sci.*, 1996, **21**, 893-950.

2 V. Percec, C. H. Ahn, G. Ungar, D. J. P. Yeardley, M. Moller and S. S. Sheiko, *Nature*, 1998, **391**, 161-164.

3 X.-F. Chen, Z. Shen, X.-H. Wan, X.-H. Fan, E.-Q. Chen, Y. Ma and Q.-F. Zhou, *Chem. Soc. Rev.*, 2010, **39**, 3072-3101.

4 J. F. Ban, S. Chen and H. L. Zhang, *Chinese J. Polym. Sci.*, 2015, **33**, 1245-1259.

5 F. Zhou, Q.-H. Zhou, H.-J. Tian, C.-S. Li, Y.-D. Zhang, X.-H. Fan and Z.-H. Shen, *Chinese J. Polym. Sci.*, 2015, **33**, 709-720.

6 V. P. Shibaev, S. G. Kostromin, N. A. Plate, S. A. Ivanov, V. Y. Vetrov and I. A. Yakovlev, *Polym. Commun.*, 1983, **24**, 364-365.

7 H. J. Coles and R. Simon, *Polymer*, 1985, **26**, 1801-1806.

8 J. Barauskas, L. Christerson, M. Wadsater, F. Lindstrom, A.-K. Lindqvist and F. Tiberg, *Mol. Pharm.*, 2014, **11**, 895-903.

9 D. H. Weinkauf, H. D. Kim and D. R. Paul, *Macromolecules*, 1992, **25**, 788-796.

10 I. M. Khan, Y. Yuan, D. Fish, E. Wu and J. Smid, *Macromolecules*, 1988, **21**, 2684-2689.

11 K. Yao, Y. Chen, L. Chen, F. Li, X. Li, X. Ren, H. Wang and T. Liu, *Macromolecules*, 2011, **44**, 2698-2706.

12 W.-B. Zhang, X. Yu, C.-L. Wang, H.-J. Sun, I. F. Hsieh, Y. Li, X.-H. Dong, K. Yue, R. Van Horn and S. Z. D. Cheng, *Macromolecules*, 2014, **47**, 1221-1239.

13 L. Chen, Y. Chen, K. Yao, W. Zhou, F. Li, L. Chen, R. Hu and B. Z. Tang, *Macromolecules*, 2009, **42**, 5053-5061.

14 D. Zhou, Y. Chen, L. Chen, W. Zhou and X. He, *Macromolecules*, 2009, **42**, 1454-1461.

15 L. Chen, Y. Chen, D. Zhou, F. Li, D. Zha and K. Yao, *Macromol. Chem. Phys.*, 2011, **212**, 24-41.

16 L. Chen, Y. Chen, D. Zha and Y. Yang, *J. Polym. Sci., Part A: Polym. Chem.*, 2006, **44**, 2499-2509.

17 H. Finkelmann, H. Ringsdorf and J. H. Wendorff, *Makromol. Chem., Macromol. Chem. Phys.*, 1978, **179**, 273-276.

18 F. Hessel and H. Finkelmann, *Polym. Bull.*, 1985, **14**, 375-378.

19 Q. F. Zhou, H. M. Li and X. D. Feng, *Macromolecules*, 1987, **20**, 233-234.

20 Q. Zhou, X. Zhu and Z. Wen, *Macromolecules*, 1989, **22**, 491-493.

21 L. Gao, Z. Shen, X. Fan and Q. Zhou, *Polym. Chem.*, 2012, **3**, 1947-1957.

22 X. Wan, F. Zhang, P. Wu, D. Zhang, X. Feng and Q.-F. Zhou, *Macromol. Symp.*, 1995, **96**, 207-218.

23 P. Gopalan and C. K. Ober, *Macromolecules*, 2001, **34**, 5120-5124.

24 D. Zhang, Y. Liu, X. Wan and Q.-F. Zhou, *Macromolecules*, 1999, **32**, 4494-4496.

25 D. Zhang, Y.-X. Liu, X.-H. Wan and Q.-F. Zhou, *Macromolecules*, 1999, **32**, 5183-5185.

26 H. Tu, X. Wan, Y. Liu, X. Chen, D. Zhang, Q.-F. Zhou, Z. Shen, J. J. Ge, S. Jin and S. Z. D. Cheng, *Macromolecules*, 2000, **33**, 6315-6320.

27 S. Chen, L.-C. Gao, X.-D. Zhao, X.-F. Chen, X.-H. Fan, P.-Y. Xie and Q.-F. Zhou, *Macromolecules*, 2007, **40**, 5718-5725.

28 S. Chen, L.-Y. Zhang, L.-C. Gao, X.-F. Chen, X.-H. Fan, Z. Shen and Q.-F. Zhou, *J. Polym. Sci., Part A: Polym. Chem.*, 2009, **47**, 505-514.

29 Q.-K. Zhang, H.-J. Tian, C.-F. Li, Y.-F. Zhu, Y. Liang, Z. Shen and X.-H. Fan, *Polym. Chem.*, 2014, **5**, 4526-4533.

30 Z. Zhu, J. Zhi, A. Liu, J. Cui, H. Tang, W. Qiao, X. Wan and Q. Zhou, *J. Polym. Sci., Part A: Polym. Chem.*, 2007, **45**, 830-847.

31 J. Cui, A. Liu, J. Zhi, Z. Zhu, Y. Guan, X. Wan and Q. Zhou, *Macromolecules*, 2008, **41**, 5245-5254.

32 C. Ye, H.-L. Zhang, Y. Huang, E.-Q. Chen, Y. Lu, D. Shen, X.-H. Wan, Z. Shen, S. Z. D.

Cheng and Q.-F. Zhou, *Macromolecules*, 2004, **37**, 7188-7196.

33 Y.-F. Zhao, X.-H. Fan, X.-H. Wan, X.-F. Chen, Yi, L.-S. Wang, X. Dong and Q.-F. Zhou, *Macromolecules*, 2006, **39**, 948-956.

34 C.-P. Chai, X.-Q. Zhu, P. Wang, M.-Q. Ren, X.-F. Chen, Y.-D. Xu, X.-H. Fan, C. Ye, E.-Q. Chen and Q.-F. Zhou, *Macromolecules*, 2007, **40**, 9361-9370.

35 P. Gopalan, L. Andruzzi, X. Li and C. K. Ober, *Macromol. Chem. Phys.*, 2002, **203**, 1573-1583.

36 S. Hilf and A. F. M. Kilbinger, *Nature Chem.*, 2009, **1**, 537-546.

37 S. V. Arehart and C. Pugh, *J. Am. Chem. Soc.*, 1997, **119**, 3027-3037.

38 C. Pugh and R. R. Schrock, *Macromolecules*, 1992, **25**, 6593-6604.

39 C. Pugh, J.-Y. Bae, J. Dharia, J. J. Ge and S. Z. D. Cheng, *Macromolecules*, 1998, **31**, 5188-5200.

40 H. Yang, F. Zhang, B.-P. Lin, P. Keller, X.-Q. Zhang, Y. Sun and L.-X. Guo, *J. Mater. Chem. C*, 2013, **1**, 1482-1490.

41 B. Geng, L.-X. Guo, B.-P. Lin, P. Keller, X.-Q. Zhang, Y. Sun and H. Yang, *Polym. Chem.*, 2015, **6**, 5281-5287.

42 H. A. Haque, S. Kakehi, M. Hara, S. Nagano and T. Seki, *Langmuir*, 2013, **29**, 7571-7575.

43 S.-K. Ahn, P. Deshmukh, M. Gopinadhan, C. O. Osuji and R. M. Kasi, *ACS Nano*, 2011, **5**, 3085-3095.

44 M.-H. Li, P. Keller and P.-A. Albouy, *Macromolecules*, 2003, **36**, 2284-2292.

45 Y.-F. Zhu, Z.-Y. Zhang, Q.-K. Zhang, P.-P. Hou, D.-Z. Hao, Y.-Y. Qiao, Z. Shen, X.-H. Fan and Q.-F. Zhou, *Macromolecules*, 2014, **47**, 2803-2810.

46 Y.-F. Zhu, X.-L. Guan, Z. Shen, X.-H. Fan and Q.-F. Zhou, *Macromolecules*, 2012, **45**, 3346-3355.

47 Y. Xu, Q. Yang, Z. Shen, X. Chen, X. Fan and Q. Zhou, *Macromolecules*, 2009, **42**, 2542-2550.

48 E. Klarmann, L. W. Gatyas and V. A. Shternov, *J. Am. Chem. Soc.*, 1932, **54**, 298-305.

**TOC Graphic for**

# Effects of Rigid Core and Flexible Tails on the Phase Behaviors of Polynorbornene-Based Mesogen-Jacketed Liquid Crystalline Polymers

Zhen-Yu Zhang, Qian Wang, Ping-Ping Hou, Zhihao Shen,* and Xing-He Fan*

Beijing National Laboratory for Molecular Sciences, Key Laboratory of Polymer Chemistry and Physics of Ministry of Education, Center for Soft Matter Science and Engineering, College of Chemistry and Molecular Engineering, Peking University, Beijing, 100871, China

The MJLCPs with a polynorbornene main chain and different side groups have been precisely synthesized for investigating the effect of side group architecture and temperature on the liquid crystalline polymer behaviors.